

Removal of accidental degeneracies in semiconductor quantum wires

J. Shertzer

Department of Physics, College of the Holy Cross, Worcester, Massachusetts 01610

L. R. Ram-Mohan

Department of Physics, Worcester Polytechnic Institute, Worcester, Massachusetts 01609

(Received 21 December 1989)

We obtain the energy levels of carriers in rectangular GaAs/Ga_{1-x}Al_xAs quantum-wire heterostructures with finite barriers using finite-element analysis. The energy spectra obtained are dramatically different from those determined analytically with use of the infinite-barrier approximation. The infinite-barrier approximation also introduces extra degeneracies in the energy spectra as a consequence of the separability of the potential. These accidental degeneracies are removed when the barrier height corresponding to the band offset of the surrounding medium is used in calculating the energy levels. Group-theory considerations of the square are used to explain the removal of these accidental degeneracies.

I. INTRODUCTION

The ability to confine electrons spatially in a controlled way in semiconductor heterostructures has led to the observation of remarkable new optical and transport properties in such structures.¹ Consequences of one-dimensional confinement in planar layered structures and the resultant quantized energy levels have been explored in great detail over the past two decades. In 1980, Sasaki² considered theoretically the consequences of growing heterostructures which would confine electrons in two dimensions, the so-called quantum wire (QW) or the two-dimensional quantum well. Since then, control over growth at an atomic level has allowed the construction of such heterostructures.³ As in one-dimensional confinement, the principal effect is to profoundly change the energy spectra of electrons which in turn influence the optical and transport properties of the composite material.⁴

In this paper we obtain the energy levels of electrons and holes in a quantum wire of GaAs with a finite confining potential arising from the band offset of the surrounding Ga_{1-x}Al_xAs medium. Earlier theoretical considerations have either assumed that the confining potential is infinite,⁵ or have used a periodic arrangement of QW's which converts the problem to the determination of narrow energy bands in a periodic structure using tight-binding models.⁶ Our results show that the energy levels for the finite potential are significantly lower than those obtained with the infinite barrier, which suggests that the infinite-barrier approximation is not valid for quantum wires. More striking, however, is the lifting of the degeneracies of certain levels of a quantum wire with square cross section when a finite-barrier potential is used in calculating the energy spectrum.

In Sec. II, the finite-element method is used to solve the Schrödinger equation in the effective-mass approximation. We give results for the carriers in

GaAs/Ga_{0.63}Al_{0.37}As for quantum wires of typical dimensions and show that certain degeneracies of the infinite square wire are lifted. In Sec. III, we use group-theoretical arguments to explain which of the degeneracies present in the infinite square well are lifted when a finite barrier is used. We investigate the dependence of the splitting of the doublets on the barrier height for heavy holes over a range of concentration x of Al in the Ga_{1-x}Al_xAs barrier.

II. FINITE-ELEMENT ANALYSIS OF THE QUANTUM WIRE

In the envelope-function approximation⁷ (EFA), the differential equation for the electron's envelope function $f(x,y)$ contains a nonseparable potential $V(x,y)$ corresponding to a finite barrier height,

$$-(\hbar^2/2m^*)(\partial^2/\partial x^2 + \partial^2/\partial y^2)f(x,y) + V(x,y)f(x,y) = Ef(x,y), \quad (1)$$

where m^* is the carrier effective mass m_w^* or m_b^* in the well or in the barrier, respectively. The potential $V(x,y)=0$ for $|x| \leq a/2$ and $|y| \leq b/2$, and $V=V_0$ outside the well of dimension $a \times b$ centered at the origin. The input parameters for the band offsets and effective masses of conduction electrons, light holes, and heavy holes in GaAs and in Ga_{1-x}Al_xAs are obtained in the same way as in the earlier investigation of the Bastard models.⁸

The finite-element method (FEM) is used to solve Eq. (1) for the energy levels as well as the eigenfunctions $f(x,y)$. The FEM is a flexible variational method and the efficacy of this method in solving quantum-mechanical problems with nonseparable potentials has been well established.⁹ The region of interest is partitioned into small elements in each of which the physical conditions of the problem hold. The unknown function

TABLE I. Conduction-electron energy levels in GaAs/Ga_{0.63}Al_{0.37}As QW's, with $m_w^* = 0.0665m_0$ and $m_b^* = 0.0858m_0$. The quantum numbers (n_x, n_y) are also indicated.

Cross-sectional area $a \times b$ (\AA^2)	Energy (meV)		Energy (meV)	
	$V_0 = 276$ meV	(n_x, n_y)	$V_0 = \infty$	(n_x, n_y)
50×50	155.3	(1,1)	452.4	(1,1)
100×50	111.1	(1,1)	282.7	(1,1)
	197.6	(2,1)	452.4	(2,1)
100×100	63.5	(1,1)	113.1	(1,1)
	155.2	(1,2)	282.7	(1,2)
	155.2	(2,1)	282.7	(2,1)
	239.6	(2,2)	452.4	(2,2)
	274.2	(1,3)+(3,1)	565.5	(1,3)

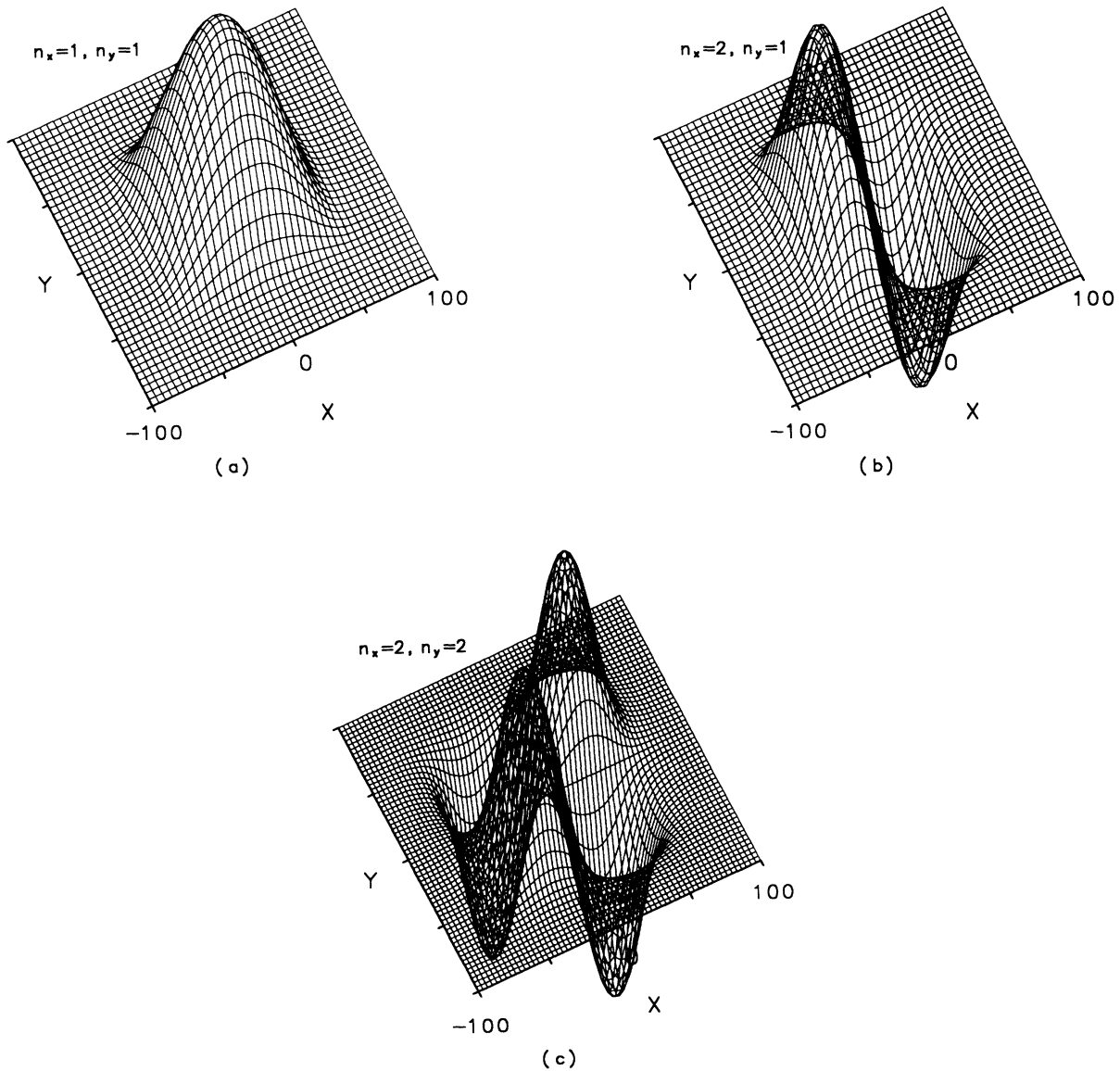


FIG. 1. Heavy-hole wave functions in a $100 \times 100 \text{\AA}^2$ QW for (a) the ground state (1,1), (b) the first excited state (2,1), and (c) the excited state (2,2).

TABLE II. Light-hole energy levels in GaAs/Ga_{0.63}Al_{0.37}As QW's, with $m_w^* = 0.0905m_0$ and $m_b^* = 0.1107m_0$.

Cross-sectional area $a \times b$ (Å ²)	Energy (meV)		Energy (meV)	
	$V_0 = 184$ meV	(n_x, n_y)	$V_0 = \infty$	(n_x, n_y)
50 × 50	110.7	(1,1)	332.4	(1,1)
100 × 50	79.8	(1,1)	207.8	(1,1)
	141.3	(2,1)	332.4	(2,1)
100 × 100	46.0	(1,1)	83.1	(1,1)
	111.7	(1,2)	207.8	(1,2)
	111.7	(2,1)	207.8	(2,1)
	171.0	(2,2)	332.4	(2,2)

in each element is approximated by local Hermite interpolation functions which have the property that the expansion coefficients correspond to the values of the function and its derivatives at select points, called nodes, in the element. The global function $f(x,y)$ is constructed by joining the locally defined interpolation functions and requiring that $f(x,y)$ and its derivatives are continuous across the element boundaries. In the FEM, it is quite easy to implement the boundary condition at the well-

barrier interface, which requires the continuity of $f(x,y)$ and continuity of the effective-mass derivative. The resultant eigenvalue problem can be solved for the energy spectra and the values of $f, \partial f / \partial x, \partial f / \partial y$, and $\partial^2 f / \partial x \partial y$ at the nodes. Details of the two-dimensional FEM are given in Ref. 9.

In Tables I–III, we give the FEM values for the energy levels of conduction electrons, light holes, and heavy holes in GaAs/Ga_{0.63}Al_{0.37}As rectangular wires of di-

TABLE III. Heavy-hole energy levels in GaAs/Ga_{0.63}Al_{0.37}As QW's, with $m_w^* = 0.3774m_0$ and $m_b^* = 0.3865m_0$.

Cross-sectional area $a \times b$ (Å ²)	Energy (meV)		Energy (meV)	
	$V_0 = 184$ meV	(n_x, n_y)	$V_0 = \infty$	(n_x, n_y)
50 × 50	46.5	(1,1)	79.7	(1,1)
	112.2	(1,2)	199.3	(1,2)
	112.2	(2,1)	199.3	(2,1)
	172.7	(2,2)	318.8	(2,2)
100 × 50	30.9	(1,1)	49.8	(1,1)
	53.1	(2,1)	79.7	(2,1)
	89.5	(3,1)	129.5	(3,1)
	97.4	(1,2)	169.4	(1,2)
	119.0	(2,2)	199.3	(2,2)
	138.2	(4,1)	199.3	(4,1)
	154.0	(3,2)	249.1	(3,2)
	182.8	(1,3) + (5,1)	288.9	(5,1)
100 × 100	15.1	(1,1)	19.9	(1,1)
	37.4	(1,2)	49.8	(1,2)
	37.4	(2,1)	49.8	(2,1)
	59.7	(2,2)	79.7	(2,2)
	74.0	(1,3) + (3,1)	99.6	(1,3)
	74.2	(1,3) – (3,1)	99.6	(3,1)
	96.2	(2,3)	129.5	(2,3)
	96.2	(3,2)	129.5	(3,2)
	123.4	(1,4)	169.4	(1,4)
	123.4	(4,1)	169.4	(4,1)
	132.2	(3,3)	179.4	(3,3)
	144.2	(2,4) + (4,2)	199.3	(2,4)
	145.9	(2,4) – (4,2)	199.3	(4,2)
	179.4	(3,4)	249.1	(3,4)
	179.4	(4,3)	249.1	(4,3)
	178.32	(1,5) + (5,1)	259.1	(1,5)
179.70	(1,5) – (5,1)	259.1	(5,1)	

mension $50 \times 50 \text{ \AA}^2$, $100 \times 50 \text{ \AA}^2$, and $100 \times 100 \text{ \AA}^2$. A conduction-band offset of $0.6\Delta E_g$ at the heterointerface was used in the calculations. Energy values reported here are accurate to within 0.1 meV. As in the case of one-dimensional quantum-well confinement, it is convenient to label the energy levels using the quantum numbers (n_x, n_y) associated with the infinite well, where n_x and n_y are the quantum numbers for the one-dimensional infinite square well in the x and y directions. The energy levels obtained using the infinite barrier approximation are also included in Tables I–III for comparison. Note that all of the energy levels are lowered from the values obtained with an infinite barrier. The effect of the finite potential is greater for small a and b and for energy levels approaching V_0 . For the $50 \times 50 \text{ \AA}^2$ QW, the single bound state of the conduction electron and of the light hole are reduced in energy by a factor of 3 from the infinite barrier result. Clearly, the infinite barrier approximation is invalid in this case.

Wave functions for three low-lying states for heavy holes in a $100 \times 100 \text{ \AA}^2$ QW are shown in Fig. 1. As expected, the FEM wave functions are similar to their infinite well analogs except that they leak out into the classically forbidden barrier region. The amount of barrier penetration increases as the energy level approaches the barrier height.

Note that the degeneracy for the (2,2) and (4,1) states of the infinite rectangular well ($100 \times 50 \text{ \AA}^2$) is removed. This degeneracy is present only in the infinite well because the energy is simply related to the dimension of the well and the quantum number, and the rectangular well was chosen to have commensurate sides. It is also interesting to note that there is a mixing of the states (5,1) and (1,3) for the finite rectangular well. The state lower in energy is predominantly (1,3), and the state which is slightly higher in energy is predominantly (5,1). At $x=0.37$ only the lower state is bound, and its energy is reported in Table III. However, at concentration $x=0.4$, both states are bound and the FEM wave functions exhibit this mixing of states. Such mixing can be expected only if two states that are close in energy have the same symmetry in x and y . Of course, this mixing will depend on the dimensions of the rectangular well.

We note that the currently available quantum wires have typical dimension of the order of 1000 \AA , in which we would expect the effect of the finite barrier to be less pronounced than in the examples shown in Tables I–III. We have calculated the energy levels of conduction electrons in the square quantum wire of 1000 \AA , using a finite barrier of 276 meV. The first few levels are lowered by about 5% from the value obtained in the infinite barrier approximation. For higher levels, the effect is accentuated as the levels approach the barrier height V_0 .

In the next section we examine the removal of certain degeneracies of the infinite-barrier-square-well spectra.

III. SYMMETRY PROPERTIES OF THE SQUARE QUANTUM WIRE

The symmetry properties of the envelope functions for the square quantum wire are governed by the symmetry

of the potential, C_{4v} . The character table for the point group C_{4v} is given in Ref. 10. The effects of the operators $\{E, C_2, 2C_4, 2\sigma_v, 2\sigma_d\}$ for this group on the function $f(x, y)$ are

$$\begin{aligned} Ef(x, y) &= f(x, y), \\ C_2 f(x, y) &= f(-x, -y), \\ C_4 f(x, y) &= f(y, -x), \\ C_4^{-1} f(x, y) &= f(-y, x), \\ \sigma_v f(x, y) &= f(-x, y), \\ \sigma_v^{-1} f(x, y) &= f(x, -y), \\ \sigma_d f(x, y) &= f(y, x), \\ \sigma_d^{-1} f(x, y) &= f(-y, -x). \end{aligned} \quad (2)$$

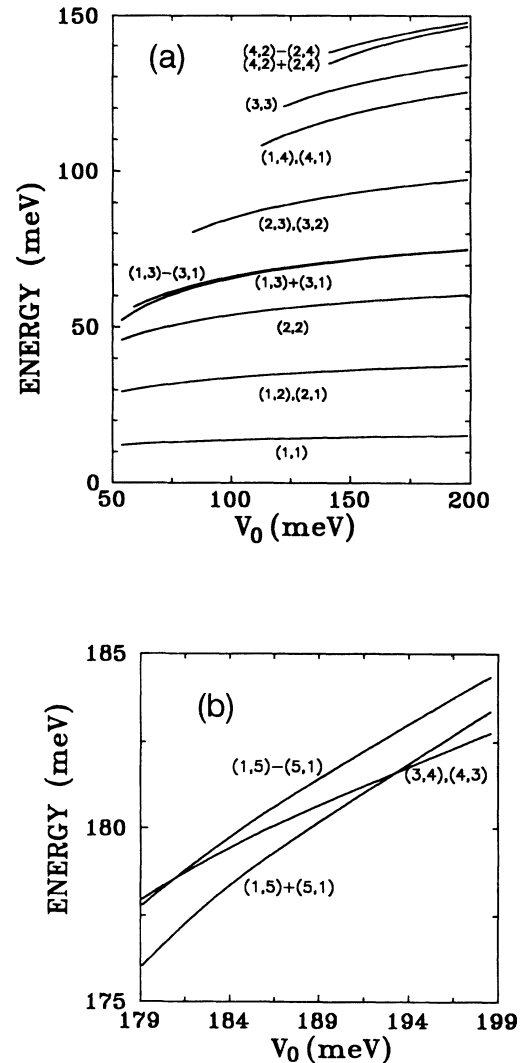


FIG. 2. The dependence of heavy-hole energy levels on the barrier height in a $100 \times 100 \text{ \AA}^2$ QW for (a) the first 10 energy levels and (b) for levels 11–13.

It is straightforward to determine the representation corresponding to the infinite-well eigenfunctions (n_x, n_y) . The (odd,odd) singlet states with $n_x = n_y$ belong to the A_1 representation and the (even,even) singlet states belong to B_2 . The degenerate states with $n_x \neq n_y$ can be classified as follows:

(even,odd) and (odd,even): E ,

(even,even): $A_2 + B_2$,

(odd,odd): $A_1 + B_1$.

Since the (even,even) and (odd,odd) degenerate states are combinations of two distinct irreducible representations, the degeneracy of these levels is not a consequence of the symmetry group of the square, but rather is due to the separability of the infinite square-well potential. Using linear combinations of the standard (n_x, n_y) eigenfunctions it is possible to construct eigenfunctions which correspond to one of the one-dimensional irreducible representations A_1 , A_2 , B_1 , or B_2 . For example, $(1,3) + (3,1)$ transforms as A_1 and $(1,3) - (3,1)$ transforms as B_1 . As we shall see, these are a more natural choice for the basis functions of this two-dimensional subspace in that they are the $V_0 \rightarrow \infty$ limit of the finite barrier eigenfunctions.

For finite barriers, the potential is nonseparable and the accidental degeneracy which was present in the infinite barrier case for the (even,even) and (odd,odd) levels is lifted (see Table III). The state that is antisymmetric about the diagonal of the square (B_1, A_2) is less bound than its symmetric counterpart (A_1, B_2). As expected, the splitting of these particular energy levels decreases as the barrier height increases, and in the limit $V_0 \rightarrow \infty$, the states are truly degenerate. In Fig. 2, we show this dependence of level splitting on barrier height for heavy holes in a $100 \times 100 \text{ \AA}^2$ GaAs/Ga $_{1-x}$ Al $_x$ As wire for the compositional range $0.1 > x > 0.4$. In some cases, the splitting of the doublet results in one state being bound, and the other free; for example, at $x = 0.1$, the state $(1,3) + (3,1)$ is bound, but $(1,3) - (3,1)$ is unbound. Also note that the energy levels for the $(1,5) \pm (5,1)$ actually cross over the $(3,4)$ level; hence, even the ordering of the energy levels is a function of V_0 .

The FEM wave functions for the square well with finite barrier are similar to their infinite barrier analogs except that there is penetration of $f(x, y)$ into the barrier region. For the degenerate states of the E representation, any two orthogonal states which span the subspace are acceptable eigenstates. In the cases where the degeneracy is removed, the wave functions for the finite barrier must correspond to a single representation as required by the group properties; the wave functions are either even or odd with respect to reflection through the diagonals. The FEM wave functions for the states $(1,3) + (3,1)$ and $(1,3) - (3,1)$ are shown in Fig. 3 over a single quadrant $(x, y \geq 0)$ for clarity of presentation; the antisymmetric state vanishes at $x = y$ as expected.

By studying the symmetry properties of the confining potential, it is straightforward to predict which of the degeneracies present in the infinite barrier approximation are due to the separability of the potential, and hence are

accidental and will be removed in the presence of a finite barrier. One can apply this analysis to the more interesting case of the three-dimensional quantum cubic dot, where the lowest 40 levels of infinite barrier spectrum have at most threefold, sixfold, ninefold, and twelvefold degeneracies. Degeneracies that arise from nonidentical quantum numbers [for example, $(2,2,5)$ and $(4,4,1)$] are

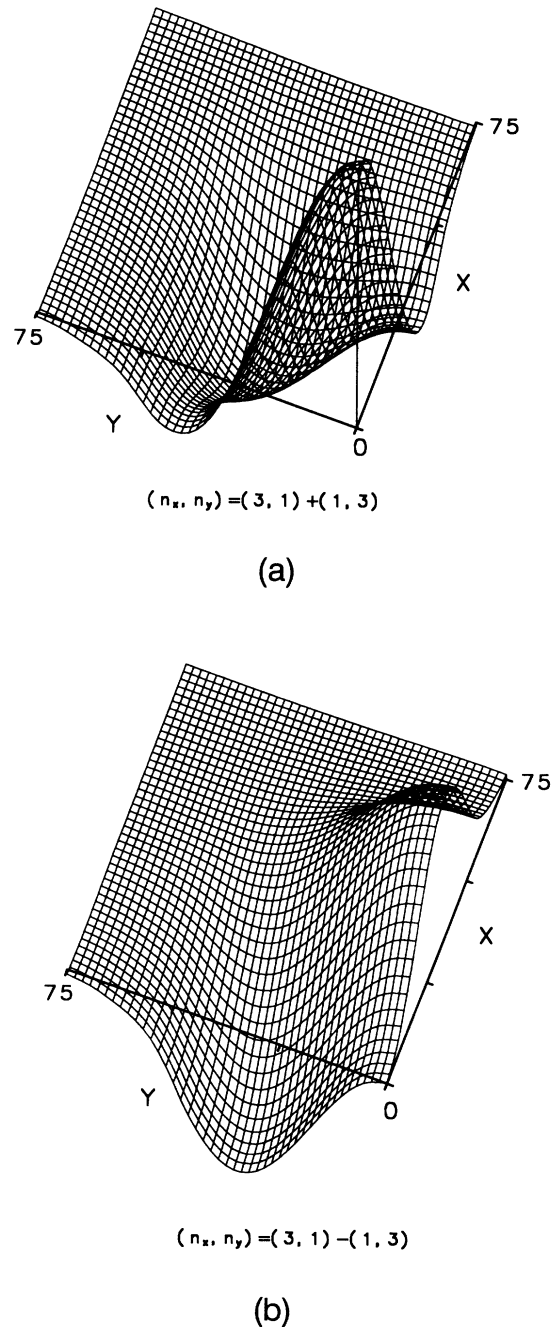


FIG. 3. Heavy-hole wave functions in a $100 \times 100 \text{ \AA}^2$ QW for (a) the excited state $(1,3) + (3,1)$ and (b) the excited state $(1,3) - (3,1)$, in the first quadrant.

automatically broken for a finite barrier since the energy is no longer simply related to the quantum numbers. The other degenerate states for the infinite barrier quantum cubic dot can be analyzed by looking at the behavior of the analytic solutions under the operations for the cubic group O_h . Since all of the representations of O_h are one-, two-, or three-dimensional,¹⁰ the energy spectra for the finite barrier quantum dot can have at most threefold degeneracies. Consequently, the spectrum for the finite barrier will contain many doublets and triplets whose splitting depends on the barrier heights. Finite element calculations for the cubic quantum dot are in progress.

IV. CONCLUSION

The FEM provides realistic numbers for the energy spectra in rectangular quantum wires. Such accuracy is crucial in the study of linear and nonlinear optical properties of semiconductor heterostructures. In particular, we show that the infinite barrier approximation is invalid and leads to serious errors in both the qualitative and quantitative aspects of the energy spectra. FEM can be

readily applied to two-dimensional confinement problems where the effective mass and the potential are more complicated functions of the coordinates; it is also possible to accommodate any cross-sectional configuration, including QW's grown on grooves. Finally, the extension of FEM to the problem of three-dimensional confinement is straightforward and our results will be forthcoming.

ACKNOWLEDGMENTS

This work was supported by the Strategic Defense Initiative of the Office of Innovative Science and Technology of the U.S. Department of Defense (SDI-ISTO) under Grant No. N00014-89-J-2038 (L.R.R), administered by the Naval Research Laboratory. We wish to acknowledge use of the Computing Centers at Worcester Polytechnic Institute, College of the Holy Cross, and the Cornell National Supercomputer Facility (CNSF). The CNSF receives major funding from the National Science Foundation (NSF) and the IBM Corporation. One of us (J.S.) would like to thank John D. Morgan III for his helpful discussions.

-
- ¹R. Dingle, in *Festkörperprobleme (Advances in Solid State Physics)*, edited by H. J. Queisser (Pergamon, Braunschweig, 1975), Vol. 15, p. 21; R. Dingle, in *Semiconductors and Semimetals*, edited by R. K. Willardson and A. C. Beer (Academic, San Diego, 1987), Vol. 24.
- ²H. Sakaki, *Jpn. J. Appl. Phys. Pt.2* **19**, L735 (1980).
- ³P. M. Petroff, A. C. Gossard, R. A. Logan, and W. Wiegmann, *Appl. Phys. Lett.* **41**, 635 (1982); J. Cibert, P. M. Petroff, G. J. Dolan, S. J. Pearton, A. C. Gossard, and J. H. English, *ibid.* **49**, 1275 (1986).
- ⁴H. Temkin, G. J. Dolan, M. B. Panish, and S. N. G. Chu, *Appl. Phys. Lett.* **50**, 413 (1987); E. Kapon, D. M. Hwang, and R. Bhat, *Phys. Rev. Lett.* **63**, 430 (1989).
- ⁵J. Lee, *J. Appl. Phys.* **54**, 5482 (1983); H. H. Hassen and H. N. Spector, *J. Vac. Sci. Technol. A* **3**, 22 (1985); H. S. Cho and P. R. Prucnal, *Phys. Rev. B* **39**, 11 150 (1989); D. A. B. Miller,

D. S. Chemla, and S. Schmit-Rink, *Appl. Phys. Lett.* **52**, 2154 (1988).

- ⁶K. B. Wong, M. Jaros, and J. P. Hagon, *Phys. Rev. B* **35**, 2463 (1987); K. S. Dy and S.-Y. Wu, *ibid.* **38**, 5709 (1988).
- ⁷G. Bastard, *Phys. Rev. B* **24**, 5693 (1981); **25**, 7584 (1982); see also L. R. Ram-Mohan, K. H. Yoo, and R. L. Aggarwal, *ibid.* **38**, 6151 (1988), and references therein.
- ⁸K. H. Yoo, L. R. Ram-Mohan, and D. F. Nelson, *Phys. Rev. B* **39**, 12 808 (1989).
- ⁹J. Shertzer, *Phys. Rev. A* **39**, 3833 (1989); J. Shertzer, L. R. Ram-Mohan, and D. Dossa, *ibid.* **40**, 4777 (1989); L. R. Ram-Mohan, S. Saigal, D. Dossa, and J. Shertzer, *Comput. Phys.* **4**(1), 50 (1990).
- ¹⁰M. Tinkham, *Group Theory and Quantum Mechanics* (McGraw-Hill, New York, 1964), pp. 325 and 329.